Design Technology for Low Thermal Expansion Materials Using 3D Printer

OYAMA Nobuyuki[*1] ASAHINA Mitsuki[*2] HANDA Takuo[*3]

Abstract:

Demand for low thermal expansion materials is increasing due to the electrification of automobiles and the increase in communication volume. Furthermore, products that have high thermal conductivity as well as low thermal expansion properties have been earnestly desired in recent years.

Metal additive manufacturing technology has made it possible to manufacture products having complicated shapes. However, there are still few reports of additive manufacturing technology using low thermal expansion materials.

The authors report the basic research results for the purpose of developing additive manufacturing technology for low thermal expansion metals. Furthermore, as an application example of the technology, we will introduce products that have the both low thermal expansion and high thermal conductivity by properly arranging position of each material.

1. Introduction

In recent years, there has been heightened demand for high accuracy in the fields of optical equipment and aerospace, and in an increasing number of cases, low thermal expansion materials have been adopted in the component parts of devices to suppress thermal deformation[1]. In particular, Invar alloys (Fe-36wt% Ni alloys) and Super Invar alloys (Fe-Ni-Co alloys) are widely used in precision parts because they exhibit excellent low thermal expansion characteristics near room temperature. On the other hand, since these materials are Fe-based alloys with a large specific gravity, material development for weight reduction is also underway[2].

Additive manufacturing technology[3, 4] is called the third processing method following cutting technology and machining technology. With the progress of process digitization, shorter delivery times, weight reduction in parts with complex shapes and fundamental improvement of material properties are expected, and several examples have been reported to date[5].

For example, Akino et al.[6] investigated a SUS316L material prepared by additive manufacturing and reported that its ductility was inferior to that of materials produced by plastic working due to defects along the melt-solidification interface. Kim et al.[7] reported that heat treatment was effective for improving the hardness and tensile strength of an additive manufacturing model of maraging steel, and Maruno et al.[8] investigated the mechanical properties of an additive manufacturing material of Inconel 718, which is a Ni-Cr-Fe-based alloy, and reported that its anisotropy was alleviated by thermal stress removal treatment. However, among materials other than SUS316, maraging steel and Inconel, the target materials were limited to Ti-6Al-4V[9] and Al-Si-Mg alloys[10], and there have been few reports on additive manufacturing technology for low thermal expansion materials.

The authors applied an additive manufacturing technology to the powder of a low thermal expansion alloy[11] (hereinafter, LEX-ZERO™) with an extremely small coefficient of thermal expansion, which was developed by our company, Nippon Chuzo K.K., and conducted a basic study on its thermal expansion characteristics, mechanical properties, anisotropy, machin-

† Originally published in *JFE GIHO* No. 47 (Feb. 2021), p. 55−61

*1 Dr. Eng.,
General Manager,
Planning and Coordination Department,
NIPPON CHUZO

*2 Staff,
Castings Technical Service and Technical Department,
NIPPON CHUZO

*3 Principal Senior Researcher,
Castings Technical Service and Technical Department,
NIPPON CHUZO

ability and aging behavior. This paper presents the results of that study and an example of an additive manufacturing model utilizing LEX-ZERO.

2. Experimental Method

2.1 Basic Experiment of Additive Manufacturing

2.1.1 Experimental sample and apparatus

Table 1 shows the chemical composition of the LEX-ZERO used in this experiment. **Figure 1** shows secondary electron images of the LEX-ZERO powder with the composition in Table 1 used in this experiment, and **Fig. 2** shows the particle size distribution and circularity of LEX-ZERO powder produced by the gas atomization method[12] using Ar. Circularity was defined as shown in Eq. (1).

$$C = 4\pi S/L^2 \quad \cdots\cdots (1)$$

Based on Fig. 1 and Fig. 2, the LEX-ZERO powder used in this study has circularity of approximately 0.8, and thus is considered to be close to spherical. The particle size of powder used here was 10 to 45 μm, which is suitable for the SLM (Selective Laser Melting) type metal lamination molding device (3D printer) used in this research.

Figure 3 shows a photograph of the appearance of the 3D printer used in the experiment. This device is equipped with a 400 W class Yb fiber laser (beam spot diameter: approximately 0.1 mm).

Table 2 shows the range of the laser irradiation conditions. As shown in **Fig. 4**, printing was performed by rotating the laser scanning direction of each layer by 67°, referring to the method proposed by Kimura et al.[13].

Table 1 Chemical composition of sample (mass%)

C	Si	Mn	Ni	Co
≦0.05	≦0.4	≦0.5	32.5～34.5	2.0～4.5

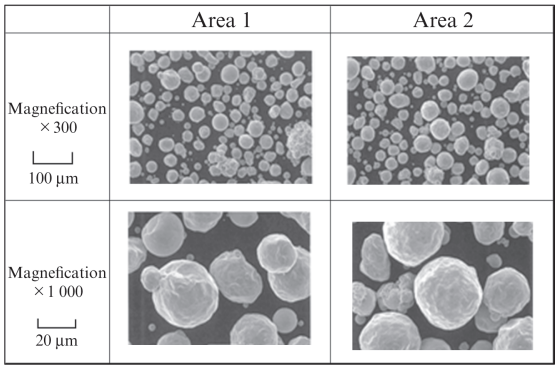

Fig. 1 SEM images of LEX-ZERO™ particles in the test

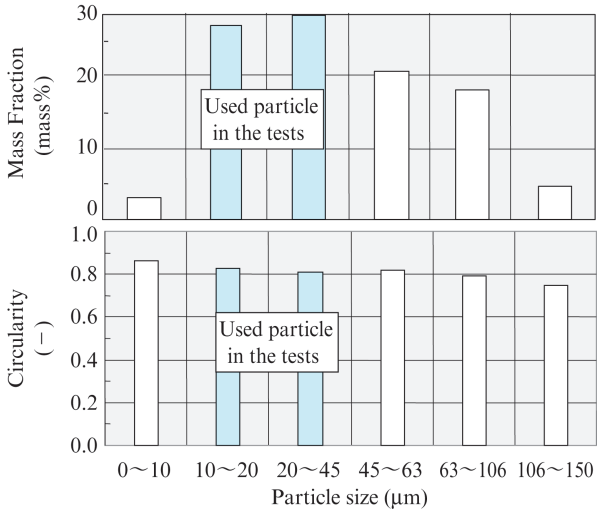

Fig. 2 Mass fraction and circularity for used LEX-ZERO™ particle produced by gas atomizer equipment

2.1.2 Measurement method

The density of the model was calculated from the weight and apparent volume of a 50 mm cube. The

Fig. 3 Appearance of 3D printer

Table 2 Laser irradiation conditions

Laser thickness (mm)	0.02-0.08
Laser power (W)	100-400
Scan spped (mm/s)	400-1 600
Scan interval (mm)	0.08-0.16

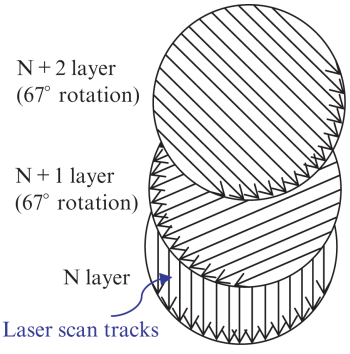

Fig. 4 Schematic diagram of laser scanning pattern[13]

coefficient of thermal expansion was measured in accordance with JIS Z 2285 with a thermal expansion meter (DIL 402 Series, manufactured by NETZSCH Co., Ltd.) using a test piece with a diameter of 8 mm × length of 50 mm, and the average coefficient of thermal expansion was calculated from the slope of the displacement in the temperature range of 10°C to 40°C. Tensile strength and other mechanical properties were measured in accordance with JIS Z 2201, and Young's modulus was measured in accordance with JIS Z 2280 (bending resonance method) using a test piece with a length of 60 mm × width of 10 mm × thickness of 2 mm. Thermal conductivity was measured by the laser flash method (TC-9000, manufactured by ULVAC-RIKO, Inc.) using a test piece with a diameter of 10 mm × thickness of 2 mm, Poisson's ratio was measured by the static measurement method (bending test), and specific heat was measured by the continuous heat insulation method (SH-3000M specific heat measurement system, manufactured by SHINKU-RIKO, Inc., current company name: ADVANCE RIKO, Inc.). The anisotropy[14] of various physical properties, which has been pointed out previously, was measured in the same direction (X-axis direction) as the lamination (printing) direction of the N-th layer, as shown in Fig. 4, the direction perpendicular to that direction (Y-axis direction) and the vertical direction (Z-axis direction) using various test pieces. A machinability test was carried out using a wet end mill (diameter: 10 mm × 4 blades).

Since it has also been noted that changes in the dimensions of SLM models occur over time[15] as a result of the carbon diffusion phenomenon, a block gauge was produced from a laminated model, and aging[16] was measured by using an optical interferometer.

2.2 SLM Application Experiment

2.2.1 Example of product weight reduction and dimensional accuracy of SLM model

As a lightweight product, a member with a truss structure, assuming an optical component support structure, was produced on a trial basis by the SLM process and compared with a conventional ordinary processed product. The dimensions at each position were measured with a CNC three-dimensional measuring machine (accuracy: ±2.3 μm/200 mm) manufactured by Mitutoyo Corporation.

2.2.2 Study on simultaneously achieving low thermal expansion and high thermal conductivity by structural design of SLM product

For the purpose of simultaneously achieving both low thermal expansion and high thermal conductivity, in this experiment, a lattice structure of the low thermal expansion material LEX-ZERO was prepared, as shown in **Fig. 5**, and a sample was produced by impregnating Cu into the cavities. Here, the volume ratio of the low thermal expansion material and the high thermal conductivity material (Cu) was 55 : 45. The coefficient of thermal expansion and the thermal conductivity of the sample were measured by the same methods as in Section 2.1.2.

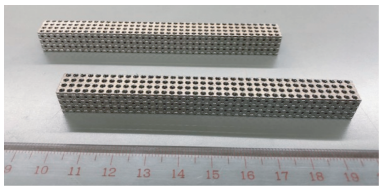

Fig. 5 Appearance of LEX-ZERO^{TM} lattice sample

3. Experimental Results

3.1 Effects of Process on Physical Properties of SLM Products of Low Thermal Expansion Alloy

Table 3 shows the thermal expansion property of LEX-ZERO and the transition temperature to the martensite phase (an index of microstructural stability at low temperature, meaning the temperature to which a low coefficient of thermal expansion can be maintained) in each of the manufacturing processes of selective laser melting (SLM), casting and forging of samples produced by each process (hereinafter, SLM product, casting product, forging product). From these results, it could be confirmed that an extremely low coefficient of thermal expansion (0.00 ± 0.19 ppm/K) can be obtained with all three manufacturing process if the alloy composition is optimized, and the transition temperature to martensite is stable in the SLM product down to at least −196°C, which is the measurable limit with liquid nitrogen.

Figure 6 show the relationship between the transi-

Table 3 Thermal expansion property of product (N = 4)

Process	Apparent density (g/cm^3)	Average thermal expansion coefficient (ppm/°C) (10～40°C)	Martensitic transformation temperature (°C)
SLM product	8.10	0.00±0.19	≦−196°C
Casting product	8.09	0.00±0.19	−30°C
Forging product	8.10	0.00±0.19	−30°C

tion temperature to martensite and the coefficient of thermal expansion at 10°C to 40°C. In the low thermal expansion material prepared by the conventional casting process, loss of low thermal expansion occurred at around −30°C, but the alloy developed in this study exhibited zero thermal expansion from room temperature to −196°C. Considering this property, application in the aerospace field is also expected.

Table 4 shows the mechanical properties of the SLM product, casting product and forging product. The tensile strength, 0.2% proof stress and Young's modulus of the SLM product were superior to those of the casting product and almost the same as those of the forging product, and elongation and the reduction of area were superior to those of both the casting product and the forging product.

Apparent density trended between 8.09 and 8.10 g/cm^3 in the products of all three process (SLM, casting, forging), as shown in Table 3, indicating that defect-free manufacturing was possible by the SLM method. Here, the input energy input per unit volume of powder melted in the SLM product is expressed by Eq. (2).

$$E = P/(v \cdot s \cdot t) \quad \cdots\cdots (2)$$

E: Energy density (J/mm^3), P: Laser output (W),
v: Laser scanning speed (mm/s),
s: Laser scanning pitch,
t: Powder layer thickness (mm)

Figure 7 shows the relationship between the input energy density and the apparent density of the model prepared by the SLM process. Since the true specific gravity of the alloy used here is estimated to be about 8.1 g/cm^3, these results confirmed that it is possible to produce products free of internal defects by the SLM method if the optimum modeling conditions are selected. Moreover, since the product density of the powder used in this study tends to saturate at an input energy of around 60 J/mm^3, it is considered that selective melting method is easier than with carbon steel for machine structural use (S15C) and is close to the selective melting condition of the AlMg10Si alloy[18]. It may be noted that not only the selective melting conditions such as the powder layer thickness, etc., but also the powder management method (powder surface condition[19] such as the contact angle, etc., number of times[20] the powder can be used repeatedly, etc.) is also important for smooth selective melting modeling.

Figure 8 shows the relationship between the Co content of the casting product and the SLM product and

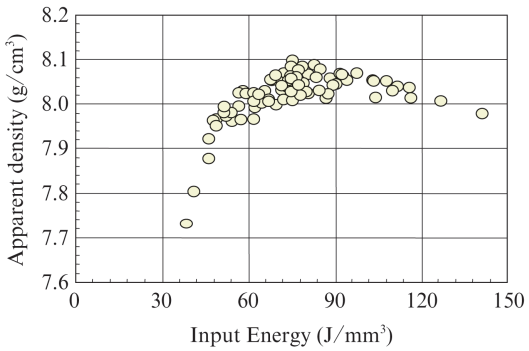

Fig. 7 Relationship between input energy and apparent density

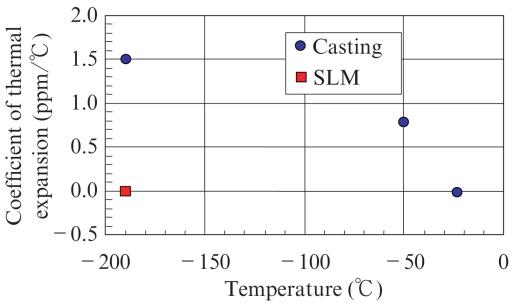

Fig. 6 Relationship between transition temperature to martensite and coefficient of thermal expansion

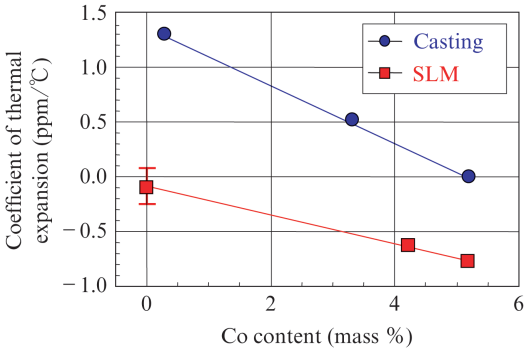

Fig. 8 Relationship between Co content and a coefficient of thermal expansion

Table 4 Mechanical property of product (N = 4)

Process	Tensile strength (MPa)	0.2% proof stress (MPa)	Elongation (%)	Aperture (%)	Young's modulus (GPa)
SLM product	479	323	45	82	131
Casting product	372	265	28	61	121
Forging product	487	334	39	75	133

the average coefficient of thermal expansion at 10˚C to 40˚C immediately after modeling. Although the coefficient of thermal expansion of both the casting product and the SLM product decreases as the Co content increases[21], that effect is slight in the SLM product, and an average coefficient of thermal expansion of 0.0 ppm/˚C could be observed even at a Co content of 0%. Since it has been pointed out that Co causes carcinogenicity and pulmonary dysfunction at levels of more than 1%, Co is regulated as a Specified Chemical Substance under Japanese law. Moreover, along with Au, Ta, W and Sn, Co is also considered to be a high-risk mineral. From this viewpoint, an alloy which ensures that the low thermal expansion property is not adversely affected if the Co content is greatly reduced is also beneficial for realizing a sustainable society.

Next, the metallographic structures were observed in order to investigate the differences among the products prepared by the casting, forging and SLM processes.

Figure 9 shows the results of observation of the macrostructures of the casting, forging and SLM products using a stereoscopic microscope, and **Fig. 10** shows the secondary electron images (SEM images). From these images, it can be understood that the structure of the SLM product is dense and homogeneous. **Figure 11** shows the relationship between the cooling rate and the measured and calculated secondary dendrite arm spacing measured from Fig. 10. In the SLM process, the melt-solidification reaction, in which the temperature of the powder deposited on the powder bed rises to more than 3 000˚C, occurs in the extremely short time of 0.01 s, and it can be inferred that the fine, uniform structure shown in Fig. 9 forms as a result of these conditions[22]. Many studies[23] to date have attempted to elucidate the melt-solidification reaction during SLM, but in the future, further research is considered necessary, in combination with metallurgical research[24] related to low thermal expansion materials.

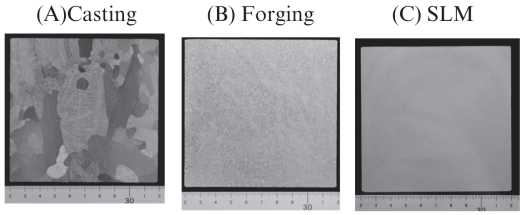

Fig. 9 Comparison in macro texture with each process

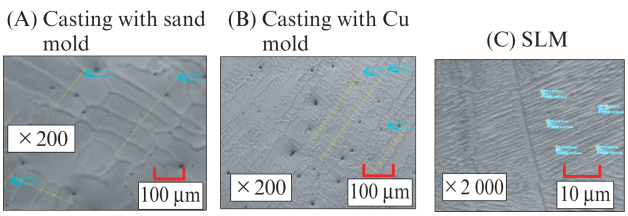

Fig. 10 Comparison of in SEM image with each process

To compare the machinability of the casting, forging and SLM products, **Fig. 12** shows the relationship between the cutting speed and cutting resistance. While the cutting resistance of the SLM product tended to be slightly lower, no significant difference was observed, and the results confirmed that the SLM product has the same level of workability as the forging and casting products.

Figure 13 shows the dimensional change of the SLM product over time. Although dimensional change of 0.07 ppm occurred at the stage of 85 days of elapsed time, this was substantially the same as that of low thermal expansion alloy castings[25].

Figure 14 shows the results of measurements of the

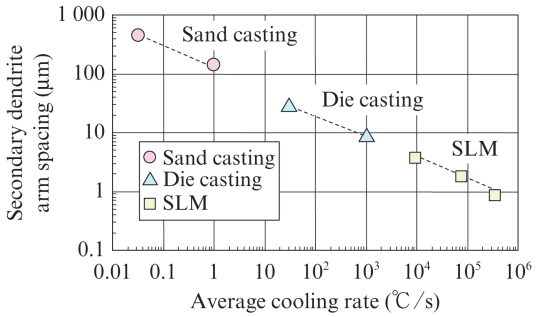

Fig. 11 Relationship between cooling rate and secondary dendrite arm spacing

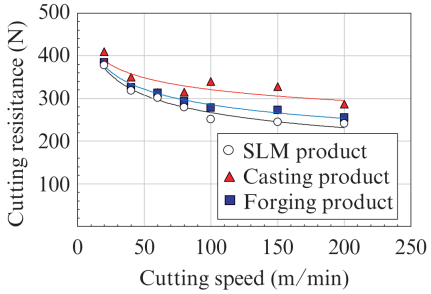

Fig. 12 Relation between cutting speed and cutting resistance for the machinability

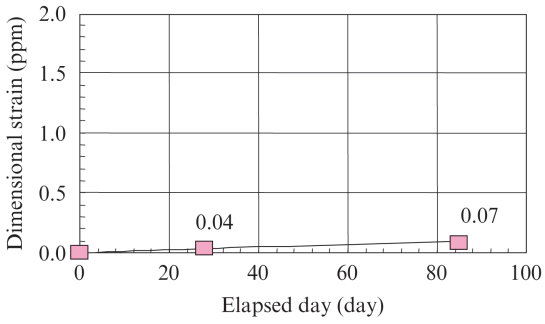

Fig. 13 Change of dimensional strain with elapsed days

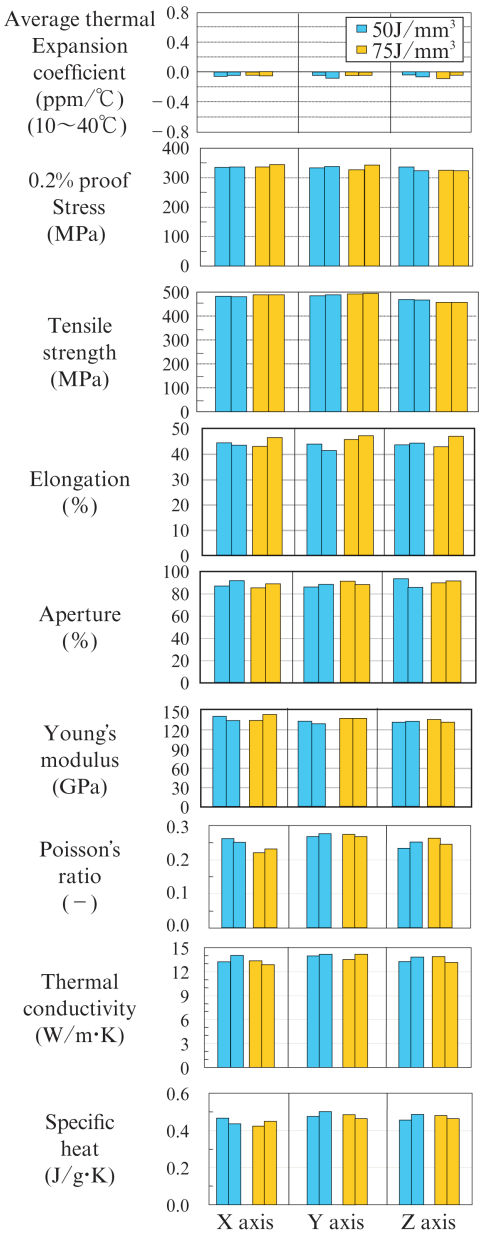

Fig. 14 Comparison in anisotropy of physical property for SLM products

anisotropy of the coefficient of thermal expansion and mechanical properties (e.g., tensile strength, etc.) of SLM products. In these measurements, the input energy was set to two levels, 50 J/mm^3 and 75 J/mm^3. Tensile strength was approximately 2% lower in the Z-axis direction, but was 25% or more higher than the 372 MPa of the casting product. Therefore, it is thought that no serious problems will occur in practical use. Among the other properties, no significant anisotropy was observed in the coefficient of thermal expansion, 0.2% proof stress, Young's modulus, elongation, reduction of area, Poisson's ratio, thermal conductivity and specific heat.

3.2 Example of SLM Product of LEX-ZERO™

Figure 15 shows an example of a lightweight product which was trial-manufactured by SLM as a truss-structured member of an optical component. In comparison with the machined product, a 40% weight reduction was successfully achieved by creating a lattice structure in the pipe part.

Figure 16 shows the relationship between the target values of the design dimensions and the measured dimensions achieved in various types of products produced by SLM. Because the modeling accuracy of all hollow parts and integrated structure products was ±200 μm or less, these results confirmed that production with high accuracy is possible, suggesting that further increases in the degree of freedom in design can also be expected in the future. In addition, it was also found that both delivery time and cost of these types of small products can be substantially reduced in comparison with the conventional machined products.

3.3 Example of Structural Design of High Functionality Material

Figure 17 shows the results of impregnation of Cu at 1 185˚C in the lattice structure produced by SLM using LEX-ZERO shown in Fig. 5, together with the results for impregnation of other elements. In this

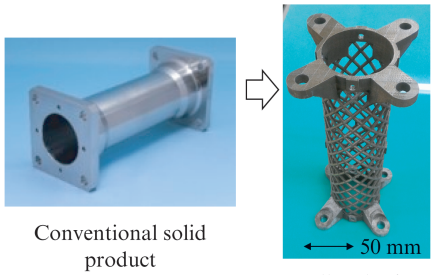

Fig. 15 Selective laser melting products of flanges simulating forged products

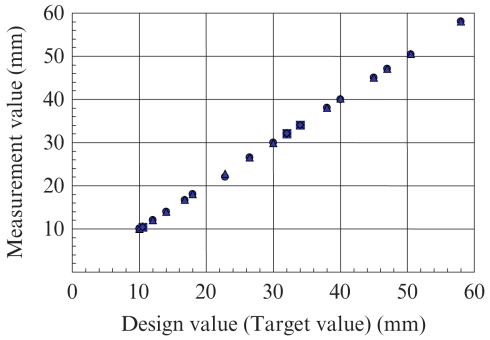

Fig. 16 Measurement results of dimensional accuracy of model products

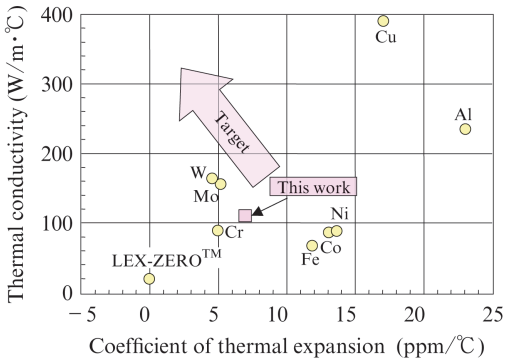

Fig. 17 Relationship between coefficient of thermal expansion and thermal conductivity

work, the volume ratio of the low thermal expansion material modeled by SLM and the high thermal conductivity material Cu was 55 : 45. In the future, the authors aim to achieve properties exceeding those of the Mo-Cu and W-Cu reported by Katsutani et al.[26] by optimizing the volume ratio and impregnation temperature.

4. Conclusion

As the result of an examination of the application of selective laser melting (SLM) technology to LEX-ZERO™, a product with an extremely low coefficient of thermal expansion developed by Nippon Chuzo K.K., the following conclusions were obtained.

1. It is possible to model SLM products with dimensional accuracy of ± 200 μm. The thermal expansion characteristics of SLM products are superior to those of casting and forging products, and mechanical properties are comparable to those of castings. The results also confirmed that SLM products are superior to cast and forged products in terms of elongation, reduction of area and other ductility characteristics.
2. By applying the SLM process to the low thermal expansion material LEX-ZERO™, mechanical strength and thermal physical properties were improved and weight reduction was easily realized. It was also found that parts with complex shapes can be manufactured at low cost.
3. The anisotropy of the various physical properties of SLM products is negligible, and virtually no secular changes were observed in the dimensions or coefficient of thermal expansion of the products.
4. There were no significant differences in the machinability of the SLM products, casting products and forging products. Therefore, it is considered that SLM products can be used in the same manner as the conventional casting and forging products up to the present.
5. It is possible to design products with complex geometries by utilizing SLM technology, and this can also contribute to product weight reduction.
6. This study demonstrated that diverse types of high functionality (high performance) products can be created by utilizing SLM technology. For example, it is possible to manufacture products that simultaneously satisfy both low thermal expansion and high thermal conductivity, which are effective for electrification of automobiles.

References

1) Jacobs, S. F. Dimensional stability of materials useful in optical engineering. Journal of Modern Optics. 1986, vol. 33, p. 1377–1388
2) Stephenson, T.; Tricker, D.; Tarrant, A.; Michel, R.; Clue, J. Physical and mechanical properties of LoVAR: a new lightweight particle-reinforced Fe-36Ni alloy. SPIE Optics + Photonics. 2015, T04.
3) Kyougoku, H. Recent Developments and Future Trends of Metal 3D Printers. Bulletin of the Iron and Steel Institute of Japan, 2019, vol. 24, no. 2, p. 697–701.
4) Ikeda, H.; Masuoka, T. Application of the Metal Additive Manufacturing Technology for Space Vehicle. Journal of the Japan Society for Precision Engineering, 2016, vol. 82, no. 7, p. 639–642.
5) Kuse, T. Introduction of 3D printer “EOS M280”. Sanyo Technical Report., 2016, vol. 23, no. 1, p. 31–33.
6) Akino, K.; Kakei, K. Strengths and Microstructure of SUS316L Fabricated by Selective Laser Melting. Journal of the Japan Institute of Metals and Materials. 2016, vol. 80, no. 12, p. 772–777.
7) Kim, D.; Kim, T.; Ha, K.; Oak, J. J.; Jeon, J. B.; Park, Y.; Lee, W. Effect of Heat Treatment Condition on Microstructural and Mechanical Anisotropies of Selective Laser Melted Maraging 18Ni-300 Steel. Metals. 2020, vol. 10, no. 3, p. 410–424.
8) Maruno, Y.; Kuwabara, K.; Pan, Wang.; Chen-Nan, S.; Hing Candice, A. K.; Jack, S. W.; Loon, A. B.; King, T. L.; Ling Sharon, N. M. A High Quality Alloy718 Powder for Powder Bed Fusion Additive Manufacturing. Hitachi Metal Technical Review. 2020, vol. 36, p. 48–57.
9) Satoh, N.; Sewatari, N.; Shimizu, T.; Nakano, Z. Real-time Observation of Melting Behavior in Selective Laser Melting of Metals. Materia Japan, 2017, vol. 56, no. 12, p. 695–698.
10) Knoop, D.; Lutz, A.; Maris, B.; Hehl, A. V. A Tailored AlSiMg Alloy for Laser Powder Bed Fusion. Metals. 2020, vol. 10, no. 4, p. 514–526.
11) Handa, T.; Kurus, N. Development of Ultra-low Thermal Expansion Casting Alloy for Precision Equipment. Sokeizai. 2014, vol. 55, no. 12, p. 28–33.
12) Okuhira, T.; Sekimoto, K. Manufacturing Processes and Characteristics of Metal Powders for Additive Manufacturing. Denki-Seiko, 2018, vol. 89, no. 1, p. 13–19.
13) Kimura, T.; Nakamoto, T. Thermal and mechanical properties of commercial-purity aluminum fabricated using selective laser melting. Journal of Japan Institute of Light Metals. 2016, vol. 66, no. 4, p. 167–173.
14) Hagihara, K.; Ishimoto, T.; Nakano, T. Creation of Anisotropic Properties by Morphology and Microstructure Control in the Additive Manufactured Metallic Materials. Materia Japan, 2018, vol. 57, no. 4, p. 145–149.
15) Steele, J. M.; Thompson, D. A.; Jacobs, S. F.; Bass, D. L. Temperature and Age Effects on Temporal Stability of In var. Proc. SPIE. 1992, vol. 40, p. 1752–1759.
16) Bitoh, Y. Calibration method of gauge block and their uncertainties. Report of the National Research Laboratory of Metrology. 2005, vol. 4, no. 1 p. 65–69.

17) Nakamoto, T. Research on high performance of shaped bjects in metal powder additive manufacturing method. Doctoral Degree Thesis Kyoto University. 2010, 109p.
18) Kyogoku, H.; Ikeshoji, T.; Yonehara, M. The Recent Trend on Additive Manufacturing Technology. Annual Report of Kinki University next generation research. 2018, vol. 9, p. 55–59.
19) Yamada, S.; Takahashi, N. Development of Evaluation Technique for Powder Bed Quality in SLM Process by Image Processing. Denki-Seiko. 2017, vol. 88, no. 1, p. 51–58.
20) Ishide, T.; Fujitani, Y.; Kuga, K.; Hatanaka, M.; Shinoki, T.; Narita, R. Development of Additive Manufacturing Technology toward Practical Utilization. Mitsubishi Heavy Industries Technical Review, 2018, vol. 55, no. 2, p. 1–7.
21) Fukamichi, K.; Saito, H. On the Magnetically Insensitive Inv ar-and Elinvar-Type Alloys, Especially on Cr-Base Alloys, Especially on Cr-Base Alloys. Bulletin of the Japan Institute of Metals. 1976, vol. 15, no. 9, p. 553–562.
22) Calta, N. P.; Wang, J.; Kiss, A.; Depond, P.; Matthews, M. J. An instrument for in situ time-resolved X-ray imaging and diffraction of laser powder bed fusion additive manufacturing processes. Review of Scientific Instruments. 2018, vol. 89, p. 1–8.
23) Kyogoku, H.; Ikeshoji, T. The Recent Trend on Additive Manufacturing Technology. Annual Report of Kinki University next generation research. 2019, vol. 10, p. 50–56.
24) Fukamichi, K. Preface for New Advances in Invar Alloys. Materia Japan, 1997, vol. 36, no. 11, p. 1064–1069.
25) Fujii, H.; Ohno, H. Zero Thermal Expansion Alloy flapping into space. Kinzoku, Agne Gijutsu Center Report. 2019, vol. 89, no. 11, p. 64–70.
26) Katsuya, H.; Yamagata, S.; Nakamura, I. History and Future Development of Heatsink Products. SEI Technical Review. 2016, vol. 188, p. 60–64.